Applied Catalysis B: Environmental 142–143 (2013) 214–221

Contents lists available at SciVerse ScienceDirect

Applied Catalysis B: Environmental

journal homepage: www.elsevier.com/locate/apcatb

Mineralization and efficiency in the homogeneous Fenton Orange G oxidation

Lucila I. Doumic[a], Patricia M. Haure[a], Miryan C. Cassanello[b], María A. Ayude[a,*]

[a] Catalizadores y Superficies, INTEMA-CONICET, Facultad de Ingeniería, UNMdP, J.B. Justo 4302, 7600 Mar del Plata, Argentina
[b] PINMATE, Dep. Industrias, FCEyN, Universidad de Buenos Aires, Intendente Güiraldes 2620, C1428BGA Buenos Aires, Argentina

ARTICLE INFO

Article history:
Received 19 October 2012
Received in revised form 16 April 2013
Accepted 26 April 2013
Available online xxx

Keywords:
Azo dye
Fenton oxidation
Intensification process

ABSTRACT

This study focuses on the homogeneous Fenton oxidation of the synthetic azo-dye Orange G as a model compound. The impact of initial TOC, hydrogen peroxide and catalyst concentrations and of temperature on mineralization and efficiency in the use of hydrogen peroxide is addressed. Dissolved oxygen concentration is monitored as an indication of the efficient use of H_2O_2 in the process. A two-stage lumped kinetic model is proposed to address the effect of initial TOC, catalyst and oxidant concentrations and temperature on total organic carbon consumption. Temperature increase and dosification of the oxidant are evaluated and compared as process intensification strategies.

1. Introduction

Nowadays, more than 100,000 dyes are available commercially and used in many industrial processes such as textile, cosmetics, food, pharmaceutical, paper, pulp manufacturing, dyeing of cloth, leather treatment, and printing. Global production exceeds 800,000 tons per year and approximately 10–15% of this production is discharged into wastewater [1]. The presence of dyes in water is decidedly undesirable since a very small amount, in some cases less than 1 ppm of dye concentration, produces obvious water coloration, may exhibit toxic effects on microbial populations and can be harmful and/or carcinogenic to mammalian animals [2]. As a result, elimination of dyes from industrial effluents before discharge is a major environmental challenge. Removal can be accomplished by different chemical and physical processes such as adsorption, coagulation, activated sludge treatment, membrane filtration, oxidations by ozone or hypochlorite. However, these methods are expensive and may not eliminate the color completely [3].

Recently, Advanced Oxidation Processes (AOPs) based on chemical oxidation were recognized as highly efficient treatments for recalcitrant wastewater [4]. Among the AOPs, Fenton's reaction is very appealing because of its simplicity and the low price, availability and small toxicity of its reagents. It is a useful technique able to degrade organic contaminants in wastewater up to a certain level of toxicity beyond which the conventional methods can be successfully used for further degradation [5]. It is generally considered [6] that in an acidic aqueous system, the reaction between ferrous ion and H_2O_2 produces hydroxyl radicals, $OH^{\bullet}$, and can involve the steps presented below:

$$Fe^{2+} + H_2O_2 \rightarrow Fe^{3+} + OH^{\bullet} + OH^{-} \quad (1)$$

$$OH^{\bullet} + Fe^{2+} \rightarrow OH^{-} + Fe^{3+} \quad (2)$$

$$Fe^{3+} + H_2O_2 \rightarrow HO_2^{\bullet} + Fe^{2+} + H^{+} \quad (3)$$

$$OH^{\bullet} + H_2O_2 \rightarrow HO_2^{\bullet} + H_2O \quad (4)$$

$$Fe^{3+} + HO_2^{\bullet} \rightarrow Fe^{2+} + O_2 + H^{+} \quad (5)$$

$$HO_2^{\bullet} + H_2O_2 \rightarrow OH^{\bullet} + H_2O + O_2 \quad (6)$$

$$Fe^{2+} + HO_2^{\bullet} \rightarrow Fe^{3+} + HOO^{-} \quad (7)$$

$$2H_2O_2 \rightarrow O_2 + 2H_2O \quad (8)$$

The hydroxyl radical is known as a strong oxidant with low selectivity which can oxidize rapidly many organic compounds [7–9], as follows:

$$RH + OH^{\bullet} \rightarrow H_2O + R^{\bullet} \quad (9)$$

$$R^{\bullet} + H_2O_2 \rightarrow \text{intermediateproducts} \quad (10)$$

* Corresponding author. Tel.: +54 223 481 6600x242; fax: +54 223 481 0046.
E-mail address: mayude@fi.mdp.edu.ar (M.A. Ayude).

0926-3373/$ – see front matter © 2013 Elsevier B.V. All rights reserved.
http://dx.doi.org/10.1016/j.apcatb.2013.04.054

$$\text{Intermediateproducts} + OH^{\bullet} \rightarrow CO_2 + H_2O + \text{inorganicsalts} \quad (11)$$

According to this, once hydroxyl radicals are formed, they can react either with an organic, leading to an oxidized species, with unreacted hydrogen peroxide or with ferrous ions, leading in this case to inactive molecular oxygen (scavenger reactions). An increase in dissolved oxygen concentration during the reaction course is then a signal of an inefficient use of hydrogen peroxide, as stated by Santos-Juanes et al. [10]. The parasitic reactions affect the overall degradation efficiency and may cause a significant increase of operational costs. The sequential addition of oxidant has been recently reported as a strategy to minimize these adverse effects and therefore improve oxidation rates in Fenton process [11–13].

Moreover, it has been shown that, although H_2O_2 is always necessary along Fenton's reaction, oxygen may replace H_2O_2, especially at high organic concentrations and/or at low H_2O_2 loads [14,15]:

$$R^{\bullet} + O_2 \rightarrow ROO^{\bullet} \quad (12)$$

$$ROO^{\bullet} + RH \rightarrow ROOH + R^{\bullet} \quad (13)$$

$$ROO^{\bullet} + H_2O \rightarrow ROH + HO_2^{\bullet} \quad (14)$$

Several attempts have been made to develop kinetic models for the Fenton process to allow the prediction of outcomes in continuous processes/reactors. Mechanistic reaction models have been proposed for formic acid and 4-chlorophenol [16,8] leading to a great number of kinetic parameters, which clearly complicates its application in reactor design. Lumped simple rate expressions may be useful for the needs of reactor design, even though they are restricted to specific organic compounds in the feed and reaction conditions. This approach has been generally applied for Fenton oxidation of dyes and organic compounds mixtures [17–19].

The aim of this work is to determine the influence of various parameters on the Fenton oxidation of the synthetic azo-dye Orange G as a model compound in the presence of air bubbling, in a semi-batch reactor. Dissolved oxygen concentration is monitored as an indication of the efficient use of H_2O_2 in the process. A two-stage lumped kinetic model is proposed to address the effect of initial TOC, catalyst and oxidant concentrations and temperature on total organic carbon consumption. The feasibility of process intensification, by increasing temperature or by splitting the oxidant dosage, is examined.

2. Experimental methods

2.1. Materials

All the chemicals used (Orange G, ferrous sulfate, H_2O_2) were analytical grade without any further purification. Deionized water was used throughout this study.

2.2. Experimental set up and procedures

Orange G oxidation tests were conducted in a batch lab-scale Erlenmeyer flask (0.2-L capacity), equipped with a magnetic stirrer (stir bar 4 cm-length). Air or nitrogen was supplied from the bottom of the batch reactor through a glass sparger tube with a 2 mm nozzle (situated at a side of the stirrer). Temperature control was ensured by means of a thermostat.

For each test, the Orange G solution (175 ml) was placed into the reactor. The pH of the reaction solution was initially adjusted to the desired value by using 1.0 M sulfuric acid or 1.0 M sodium hydroxide, and was measured with a pH-meter (HANNA instruments). The stirring speed used in experiments was 500 rpm. Air or nitrogen was bubbled at a constant flow rate of 350 ml/min. The reactions were initiated by adding calculated amounts of hydrogen peroxide and ferrous sulfate to the reactor. Liquid samples were taken out periodically and analyzed at once. The total (cumulated) volume reduction of reaction solution was always less than 10%.

Theoretical mineralization of Orange G would be given by:

$$C_{16}H_{10}N_2Na_2O_7S_2 + 42H_2O_2 \rightarrow 16CO_2 + 45H_2O + 2HNO_3 + 2NaHSO_4 \quad (15)$$

The oxidant to dye concentration ratio of the experiments was established considering the theoretical stoichiometric ratio arising from Eq. (15).

2.3. Analytical methods

The discoloration was evaluated at 492 nm using a SHIMADZU UV-1800 spectrophotometer (sample of 1 ml diluted 1:3). To assess mineralization, total organic carbon (TOC) was measured using a SHIMADZU TOC-V CPN Total Organic Carbon analyzer (sample of 1 ml diluted 1:10). Dissolved oxygen concentration (DO) was continuously measured by means of an oxygen probe provided with temperature compensation (Mettler Toledo InLab605-ISM). Hydrogen Peroxide concentration was determined by a Glycemia enzymatic test (Wiener Lab.) (sample of 20 μl). Since the reaction could continue after sampling, the whole procedure of sampling and measuring the absorbance, TOC, peroxide concentration and pH was always finished in less than 1.5 min.

Results presented here represent the average of at least three identical experiments. Reproducibility was within 6%.

Experiments were repeated to address the extent of Fe precipitation. Total iron concentration was measured with the HACH FerroVer method at the end of each run with and without filtering the samples. Initial total Fe content is coincident with that measured at 180 min in samples without filtering. The percentage of total Fe precipitated is calculated and reported as "%Fe precipitated".

The percentage of dye color removal and TOC conversions were evaluated as follows:

$$\%\text{Colour removal} = \left(1 - \frac{A_{dye}}{A_{dye,0}}\right) \times 100 \quad (16)$$

$$X_{TOC} = \left(1 - \frac{TOC}{TOC_0}\right) \times 100 \quad (17)$$

where A_{dye} and TOC are dye absorbance and total organic carbon concentration at a given time and suffix 0 indicates the initial value.

The net oxygen reaction rate (r_{O2}) represents the difference between oxygen generation rate ($r_{O2,G}$) through reactions (5), (6) and (8) and the oxygen consumption rate ($r_{O2,C}$) by reaction (12). This net oxygen reaction rate can be evaluated from experimental DO measurements as:

$$r_{O2} = r_{O2,G} - (-r_{O2,C}) = \frac{dO_2}{dt} - k_La \cdot (O_2^* - O_2) \quad (18)$$

where O_2 and O_2^* are the dissolved oxygen concentration measured along the reaction and oxygen solubility, respectively. The overall volumetric gas–liquid mass transfer coefficient (k_La) was measured in situ following the dynamic method [20]. The values obtained with air bubbling are 0.0963 min^{-1} at 25 °C and 0.1793 min^{-1} at 50 °C.

The efficient use of H_2O_2 for mineralization, or the importance of parasitic reactions can be evaluated considering the ratio between

Table 1
Explored conditions and outcomes attained at 180 min.

Run #	pH_0	T (°C)	Fe_0^{2+} (mM)	$H_2O_{2,0}$ (mM)	TOC_0 (mM)	$H_2O_{2,0}/OG_0$	$H_2O_{2,0}/Fe_0^{2+}$	X_{TOC}	$X_{H_2O_2}$	% Fe precipitated	ε
1	3	25	0.46	12	4	48	26	46	97	–	3.6
1b	6.3	25	0.46	12	4	48	26	43	98	1	3.5
2	3	25	0.46	22	4	88	48	48	88	–	1.1
3	3	25	0.46	22	8	48	48	34	67	–	3.4
4	3	25	0.69	18	6	48	26	38	94	–	0.7
5	3	25	0.91	22	4	88	24	53	100	–	1.0
5b	6.3	25	0.91	22	4	88	24	52	100	2	1.0
6	3	25	0.91	22	8	48	24	45	98	–	2.2
7	3	35	0.46	22	4	88	48	51	98	–	0.8
8	3	50	0.46	12	4	48	26	58	100	–	2.5
9	3	50	0.46	22	4	88	48	57	100	3	0.9
9b	6.3	50	0.46	22	4	88	48	49	100	7	0.7
10	3	50	0.91	22	4	88	24	60	100	4	0.9
10b	6.3	50	0.91	22	4	88	24	53	100	18	0.8
11	3	25	0.092	12	4	48	130	23	41	–	–
12	3	25	0.46	3	4	12	7	15	100	–	–
13	3	25	0.46	6	4	24	13	32	100	–	–
14	3	50	0.46	6	4	24	13	33	100	–	–

the TOC consumption rate and the oxygen generation rate, taking into account that oxygen is generated by parasitic undesirable reactions, which consume hydrogen peroxide preventing its use for generating new radicals. However, as only the net oxygen reaction rate can be calculated from experimental DO profiles, the efficiency will be approximated as follows:

$$\varepsilon = \frac{r_{TOC}}{r_{O2,G}} = \frac{r_{TOC}}{[r_{O2} + (-r_{O2,C})]} \cong \frac{r_{TOC}}{r_{O2}} \quad (19)$$

This approximation would be strictly valid for cases in which $r_{O2,C}$ can be neglected; i.e., when the oxygen generation mostly determines the dissolved oxygen concentration. This is more likely to occur for wastewaters with relatively low organic content or for high ratios of hydrogen peroxide to organics concentrations. Otherwise, when a significant consumption of oxygen occurs along the reaction time and dissolved oxygen concentration becomes lower than the solubility value, it should not be applied.

Given that instantaneous velocities contain significant uncertainty in their determination, the ratio of the mean velocities during the experiment has been considered to calculate the efficiency. Mean velocities have been evaluated by integrating the rates along the 180 min of reaction time course.

3. Results and discussion

3.1. Effect of operational variables on Orange G discoloration, mineralization and efficiency

Experiments with air or nitrogen bubbling were performed and outcomes were practically identical. This is in agreement with Utset et al. [14], who found no significant differences between experiments under different oxygen or air flow rates. Differences between air and N_2 bubbling were found mainly in DO profiles at the beginning of the run. Oxygen generation mostly determines the DO profile under nitrogen bubbling, thus oxygen is always present except at the beginning of the experiment. Air bubbling is not really necessary to improve mineralization, but a constant gas flow allows straight comparison between experiments performed under air and N_2 bubbling and contributes to eliminate mass transfer limitations.

As expected, runs performed without H_2O_2 with and without air bubbling, did not show changes in discoloration, mineralization or DO. These results indicate that oxygen does not oxidize organic compounds and organic radicals are formed only if hydrogen peroxide is present.

Experiments with oxidant concentration well below, well above and near the theoretical stoichiometric amount needed to completely mineralize the initial Orange G concentration (OG_0) were performed under air bubbling. Table 1 summarizes the explored operating conditions in terms of initial pH, temperature, initial TOC, oxidant and catalyst concentrations (pH_0, T, TOC_0, H_2O_{20}, Fe_0^{2+}, respectively). The initial molar TOC refers to the carbon content in the fresh Orange G aqueous solution. Temperature was varied between 298 and 323 K. TOC and H_2O_2 conversions, %Fe precipitated and oxidant efficiency attained at 180 min are also included in Table 1. Most of the experiments were performed at initial pH = 3, which is within the optimum range reported in literature for homogeneous Fenton oxidation [6,21]. The uncontrolled pH remains almost constant along the reaction in all the experiments.

Although the cost of Fenton processes is mostly associated to the hydrogen peroxide, the amount of acid used to bring down the pH to 3 and the amount of alkali needed to add before sending this effluent to a post treatment should be considered in the total cost of the treatment process. Therefore, experiments at natural pH of Orange G solution (pH_0 = 6.3) were performed (Table 1). In all experiments with initial pH = 6.3, pH decreased to around 3 within the first 5 min after the addition of H_2O_2 and $FeSO_4$. This pH reduction has been also observed by Gallard et al. [22] and Utset et al. [14], who stated that is a consequence of the following reaction:

$$2FeOH^+ + H_2O_2 + 2H_2O \rightarrow 2Fe(OH)_3 + 2H^+ \quad (20)$$

Iron precipitation was evidenced in all experiments performed at pH_0 = 6.3 (Table 1). Besides, elemental steps, such as reactions (3) and (5), and the oxidation of organic material into organic acids may also contribute.

Discoloration and H_2O_2 profiles are almost not affected by initial pH, but a decline in TOC conversion is observed in runs performed at higher initial pH. This decrease is more markedly in experiments performed at 50 °C. The trend may be due to the enhanced formation of insoluble ferric hydroxides at higher pH_0 and temperature (see Table 1).

Fig. 1a and b presents the temporal evolution of UV–visible absorption spectra corresponding to runs #13 and #14 performed at 25 and 50 °C, respectively. Similar trends were observed for all experiments. The disappearance of the peak at 492 nm observed in the UV–visible absorption spectra indicates that Orange G discoloration is complete. This can be explained considering that ferrous ions react very quickly with hydrogen peroxide to produce large amounts of hydroxyl radicals (Eq. (1)), which first attack azo groups and open the N=N bonds. Thus, a large amount of organic radicals ($R^\bullet$) are formed during the first minutes (Eq. (9)).

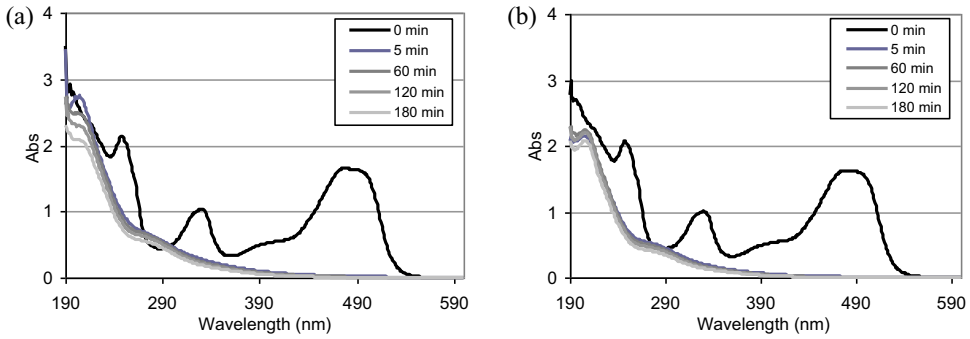

Fig. 1. UV–visible spectra. (a) Run #13 and (b) run #14.

The peak at 331 nm, characteristic of naphthalene rings, almost disappears and the absorption peak at 248 nm, characteristic of the benzene ring structure, is significantly reduced during the first minutes. The remnant peak at about 200 nm is also related to aromatic structures and is the only region that is influenced by temperature during the first minutes of reaction. Besides, various aliphatic and carboxylic acids have been reported in literature as intermediates for Orange G oxidation [3]. Complete discoloration is almost instantaneous for all the explored conditions, aside from experiment #12 in which 87% and 98% is discolorized at 1 min and 180 min, respectively. Complete and instantaneous discoloration of Orange G attained through homogeneous Fenton is not usually reported in the literature. Sun et al. [21] measured much lower Orange G discoloration rates working with $H_2O_{2,0}/OG_0$ between 90 and 500, $H_2O_{2,0}/Fe_0^{2+}$ = 285 and pH = 4.0 at 20 °C. Ramirez et al. [23] stated that, under some conditions, very high H_2O_2 concentration values enhance parasitic reactions leading to a decrease in the final discoloration.

Frequently only the dye discoloration rate is reported in the literature. However, complete discoloration of the solution does not mean that the dye is totally mineralized, so the TOC of the reaction mixture must be assessed along the reaction. Figs. 2 and 3 show the temporal profiles of TOC and oxidant concentration, respectively.

At 25 °C, when oxidant concentration is above the theoretical stoichiometric amount, a higher initial H_2O_2 concentration does not modify significantly the TOC removal (compare experiments #1 and #2). Although H_2O_2 decomposition is enhanced and theoretically more HO• radicals are produced (Eq. (1)), the increase of H_2O_2 favors parasitic reactions through reactions 4 and 6 and the efficiency decreases.

On the other hand, if H_2O_2 concentration is far below the theoretical stoichiometric dose, as in experiments #12 and #13, the oxidant is completely consumed (Fig. 3b) and the oxidation proceeds mainly via Eq. (12). Besides, hydroxyl radicals are not enough and mineralization only reaches 15% and 32%, respectively (Fig. 2b). Analogous outcomes are attained in experiment #11, where the catalyst concentration is low and the oxidant is no further consumed beyond 90 min (Fig. 3a).

The comparison between experiments #1 and #5 highlights that TOC conversion can be improved with higher catalyst and oxidant concentrations (Fig. 2a). These benefit both TOC and oxidant consumption, but the efficiency decreases. Although more hydroxyl radicals are generated, they are also consumed by parasitic reactions. Indeed, if both hydrogen peroxide and catalyst concentrations are further increased, at a given $H_2O_{2,0}/Fe_0^{2+}$ ratio, scavenger reactions will become even more important and thus, the TOC oxidation rates will diminish. This detrimental effect has been observed by Ramirez et al. [23] in the Fenton oxidation of Orange II.

The comparison between runs #2 vs. #3 and #5 vs. #6 in Table 1, outlines that increasing the initial organic concentration, increases TOC consumption rates (not conversion) since the probability of reaction between organic and oxidizing species also increases. This fact is in agreement with Burbano et al. [24]. Oxidant consumption is reduced when TOC_0 is increased to 8 mM. More radicals OH• react with the Orange G and the extent of H_2O_2 consumption in Eq. (4) and (6) may be reduced, resulting in slower degradation of the hydrogen peroxide. Then, the efficiency in the use of H_2O_2 is enhanced as seen in Table 1. Bach et al. [25] also observed this trend in the Fenton-like oxidation of phenol. It is worth mentioning that H_2O_2 decomposition is not frequently reported in literature regarding organic Fenton oxidation.

The effects of oxidant and catalyst concentrations on mineralization were also investigated at 50 °C (Table 1). Outcomes trends are analogous to those achieved at 25 °C. Oxidant concentration

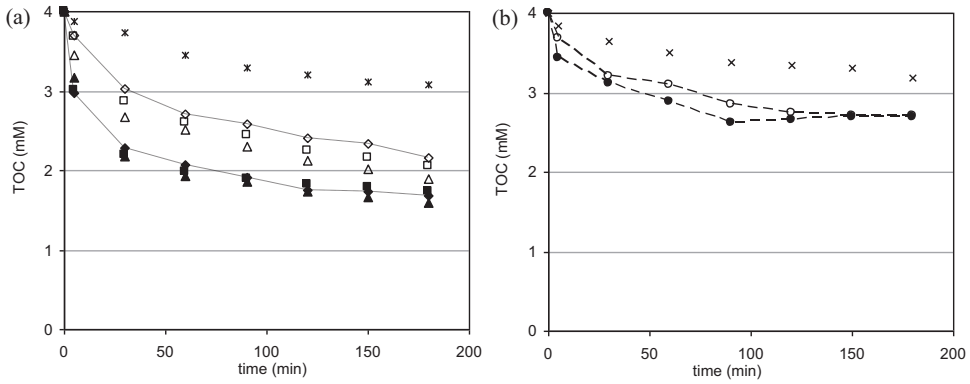

Fig. 2. TOC concentration against time at 25 °C (empty symbols) and 50 °C (solid symbols) under air flow rate. OG_0 = 0.25 mM, (a) (◇, ◆) runs #1 and #8; (□, ■) runs #2 and #9; (Δ, ▲) runs #5 and #10; (*) run #11; (b) (×) run #12; (○, ●) runs #13 and #14.

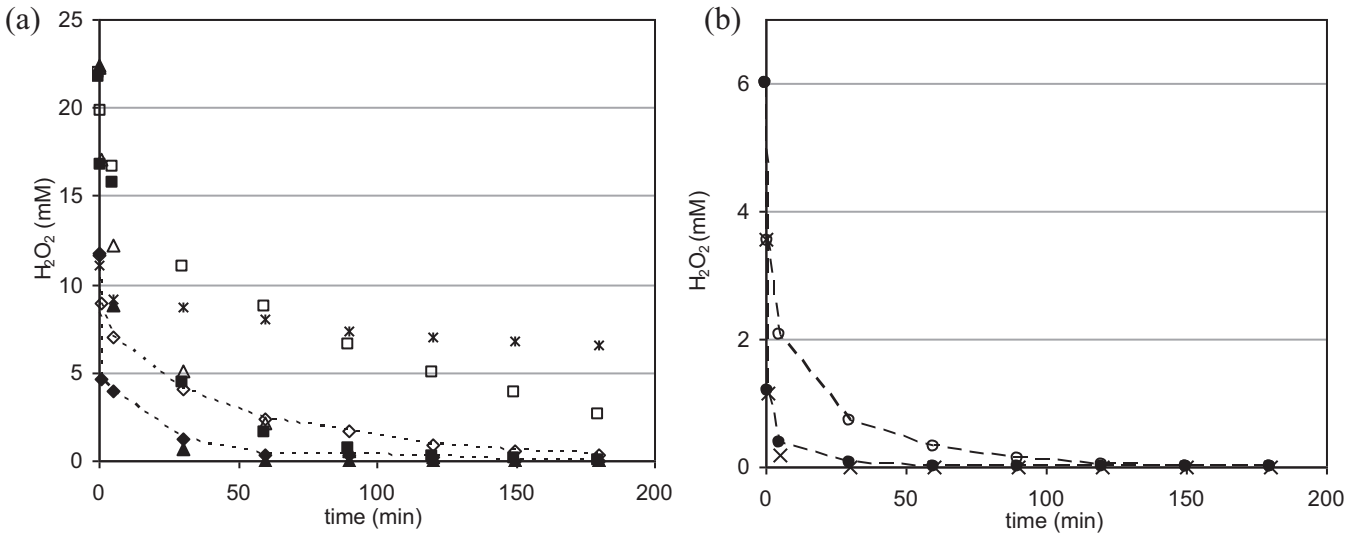

Fig. 3. Hydrogen peroxide concentration against time at 25 °C (empty symbols) and 50 °C (solid symbols) under air flow rate. OG_0 = 0.25 mM. (a) (-◇-, -◆-) runs #1 and #8; (□, ■) runs #2 and #9; (△, ▲) runs #5 and #10; (*) run #11; (b) (×) run #12; (○, •) runs #13 and #14.

profiles presented in Fig. 3a indicate that higher catalyst, oxidant concentration and temperature enhance oxidant decomposition. Fig. 2a clearly illustrates that mineralization rate is mainly enhanced by the reaction temperature, especially during the first minutes. This is in agreement with Zazo et al. [26] who studied the effect of this parameter working with the stoichiometric H_2O_2 dose. Even if higher temperature is positive to improve mineralization rate during short periods, prolonged processes can lead to a decrease in efficiency arising from the enhancement of parasitic reactions (Table 1).

On the other hand, temperature does not significantly improve the overall process when the oxidant concentration is below the stoichiometric value, as shown for experiments #13 and #14 (Fig. 2b). At 50 °C, H_2O_2 is completely consumed within 90 min and TOC is not further oxidized since the hydroxyl radicals concentration is insufficient.

Results can be further interpreted through DO profiles. Fig. 4 presents the evolution of dissolved oxygen concentration profiles attained in different experiments under air bubbling. Typically, at t = 0, the oxygen concentration equals the saturation value (O_2^*) at the operating temperature. Then, the DO decreases given that consumption rate through Eq. (12) is greater than the supply source of oxygen (generation rates and transport from air). At the minimum value of DO, these terms are equal and then, DO increases up to a maximum value since oxygen generation prevails. The concentration of organic radicals R• is small compared to hydroxyl radicals and therefore Eq. (12) does not prevail over Eqs. (4)–(6) [10]. Then, dissolved oxygen concentration slowly returns to the solubility value since main reactions do not involve oxygen generation. Under certain conditions, initial oxygen consumption is not observed and DO increases from the initial solubility value [10].

DO profiles in Fig. 4a highlights that the extension of oxygen consumption is reduced until its disappearance when higher initial catalyst and oxidant concentrations are employed and theoretically more hydroxyl radicals are formed. A higher production of OH•, as discussed previously, seems to improve TOC consumption and to a greater extent, oxygen generation rates, decreasing therefore the efficiency in the use of the oxidant.

As initial TOC concentration increases, less oxygen is formed through scavenger reactions, as seen in Fig. 4a and b. This is in line with the prevalence of the reactions between hydroxyl radicals and organic intermediates.

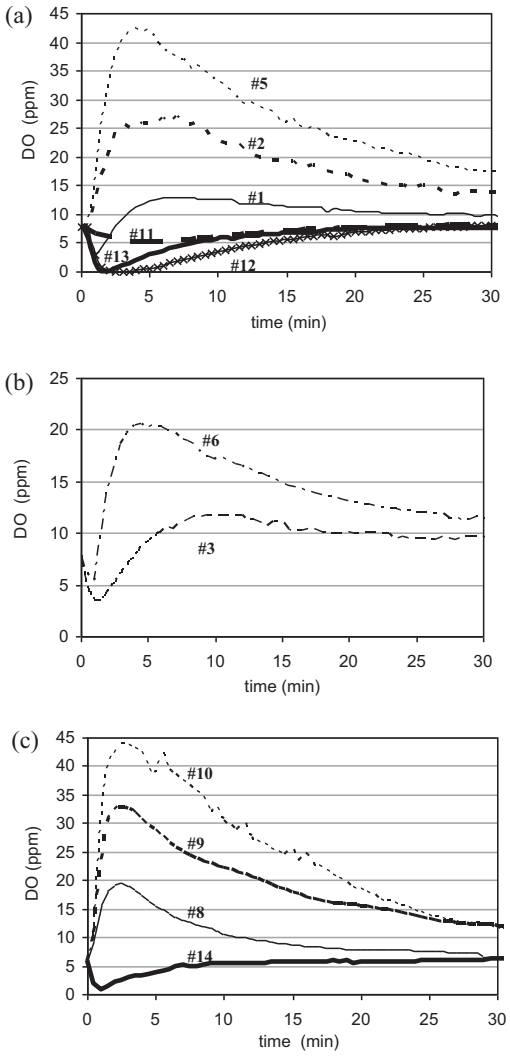

Fig. 4. DO against time for different experiments. Profiles at (a) 25 °C, OG_0 = 0.25 mM; (b) 25 °C, OG_0 = 0.5 mM; (c) 50 °C, OG_0 = 0.25 mM.

DO profiles attained at 50 °C are presented in Fig. 4c. Even though oxygen solubility decreases and mass transport to air is enhanced at higher temperature, the dissolved oxygen concentration measured during the first minutes of reaction is higher. So generation of oxygen is greater since temperature induces a faster generation of $OH^{\bullet}$ and, as discussed previously, not only TOC consumption but parasitic reactions are favored.

Dissolved oxygen profiles mainly governed by oxygen consumption indicate a lack of hydrogen peroxide and/or catalyst. This would affect negatively the mineralization rate (experiments #3, #11–#14) since reaction proceeds mainly via Eq. (12) and there are not enough hydroxyl radicals to achieve further mineralization.

3.2. Kinetic model for Fenton oxidation of Orange G

Profiles in Fig. 2 depict that the oxidation of Orange G and intermediates proceeds in a two-stage reaction: the azo dye is degraded very quickly in the first 5–10 min (Fe^{2+}/H_2O_2 stage), and then proceeds at a slower reaction rate (Fe^{3+}/H_2O_2 stage). This has been widely reported in the literature associated with the complex Fenton's process [18,19,21,24].

The influence of temperature and of the initial concentrations of dye, hydrogen peroxide and catalyst on mineralization during these two stages is analyzed trough a lumped model. Multivariate linear regressions are performed using the software package Statistical Analysis Data R [27]. The model is validated within the range of conditions studied in experiments #1–#10, in which $H_2O_{2,0}/OG_0 > 42$, $H_2O_{2,0}/Fe_0^{2+}$ between 24 and 48 and $pH_0 = 3$.

3.2.1. Fe^{2+}/H_2O_2 stage

Initial TOC removal rate ($r_{TOC,0}$) was estimated following the procedure proposed by Wu et al. [19]. The plot of the ratio of (time)/(X_{TOC}) against time ($R^2 > 0.98$), gives a straight line with intercept "a" and slope "b", where $(-r_{TOC,0}) = TOC_0/a$. It is assumed that the initial TOC consumption rate obeys the general rate equation:

$$-r_{TOC,0} = k_0(T) \cdot (TOC_0)^{x_0} \cdot (H_2O_{2_0})^{y_0} \cdot (Fe_0^{2+})^{z_0} \quad (21)$$

Then, taking logarithm and rearranging yields:

$$\ln(-r_{TOC,0}) = \ln(k_0(T)) + x_0 \ln(TOC_0) + y_0 \cdot \ln(H_2O_{2_0}) + z_0 \cdot \ln(Fe_0^{2+}) \quad (22)$$

Data at a given temperature is fitted by a multivariate linear regression and reaction orders are determined: $x_0 = 1$, $y_0 = 0$, $z_0 = 1$ (Adjusted R-square = 0.9929 and p-value = 0.0035). Then, the values of k_0 for each temperature are fitted with the Arrhenius model. Results are presented in Table 2.

3.2.2. Fe^{3+}/H_2O_2 stage

Besides Fenton's mechanism complexity, it can be assumed that Fenton's mineralization is governed by Eq. (9). Thus,

$$-r_{TOC} = k \cdot OH^{\bullet} \cdot TOC^n \quad (23)$$

Since hydroxyl radical is highly reactive, its concentration takes a steady-state value during the process and this expression can be simplified as follows:

$$-r_{TOC} = k_1' \cdot TOC^n \quad (24)$$

Table 2
Fitting parameters. Experiments 1–10 are included.

	T (°C)	k_0 ($mM^{-1}\,min^{-1}$)	Ea (kJ/mol)	R^2
Fe^{2+}/H_2O_2 stage	25	0.0313 ± 0.0052		
	35	0.0545 ± 0.0027	34.06	0.988
	50	0.0917 ± 0.0122		
	T (°C)	k_1 ($mM^{2.5}\,min^{-1}$)	Ea (kJ/mol)	R^2
Fe^{3+}/H_2O_2 stage	25	0.0100 ± 0.0013		
	35	0.0111 ± 0.0006	7.84	0.999
	50	0.0128 ± 0.0002		

In all experiments, the data taken beyond 30 min of reaction fits better a second order kinetics ($R^2 > 0.98$). In addition, following the approach of Ramirez et al. [18] for the Orange II discoloration, it is proposed that $k_1' \cdot$ depends on temperature, on the initial concentrations of H_2O_2 and Fe^{2+}, and also on the concentration of scavenger species present in the reaction mixture that depends on the initial organic concentration; then:

$$k_1' = k_1(T) \cdot (TOC_0)^{x_1} \cdot (H_2O_{2_0})^{y_1} \cdot (Fe_0^{2+})^{z_1} \quad (25)$$

Taking logarithm and rearranging yields:

$$\ln(k_1') = \ln(k_1(T)) + x_1 \cdot \ln(TOC_0) + y_1 \cdot \ln(H_2O_{2_0}) + z_1 \cdot \ln(Fe_0^{2+}) \quad (26)$$

Again, data at a given temperature is fitted by a multivariate linear regression. The reaction orders resulted: $x_1 = -1.7$, $y_1 = 0$, $z_1 = 0.2$ (Adjusted R-square = 0.9949 and p-value = 0.0026). Then, the values of k_1 are well fitted with the Arrhenius model. Results are also included in Table 2.

The order x_1 (−1.7) is in agreement with Ramirez et al. [18], who found a negative effect of the initial TOC concentration on the apparent kinetic constant for the Fe^{3+}/H_2O_2 stage in the Fenton oxidation of Orange II (−0.67).

From a practical point of view, with the aim of providing a mathematical tool to predict mineralization rate in continuous reactors, an extent of 10 min is assigned to the Fe^{2+}/H_2O_2 stage. The predicted TOC concentration at 10 min is considered as the "*initial*" value for the second stage. Experimental data is satisfactorily predicted by the proposed model as it is shown in Fig. 5 and the global error is estimated in 3%.

To sum up, TOC consumption rate can be depicted by:

$$\begin{cases} 0 < t \le 10\ \text{min} & -r_{TOC,0} = 30485 \cdot e^{(-34.06\,kJ/mol)/R\cdot T} \cdot (Fe_0^{2+})^1 \cdot (H_2O_{2_0})^0 \cdot (TOC_0)^1\ mM\,min^{-1} \\ t > 10\ \text{min} & -r_{TOC} = 0.237 \cdot e^{(-7.84\,kJ/mol)/R\cdot T} \cdot (Fe_0^{2+})^{0.2} \cdot (H_2O_{2_0})^0 \cdot (TOC_0)^{-1.7} \cdot (TOC)^2\ mM\,min^{-1} \end{cases}$$

The activation energy value obtained for the first stage is in agreement with the one reported for the discoloration of Orange G by Fenton oxidation: 34.84 kJ/mol [21]. The comparison of the activated energy values estimated for each stage confirms that temperature influences mainly the Fe^{2+}/H_2O_2 stage. This model highlights the negligible effect of initial oxidant concentration in this range of operating conditions.

3.3. Oxidant dosification

Up to this point, it can be concluded that an adequate amount of hydroxyl radicals should be generated during the first minutes of reaction to attain complete and instantaneous discoloration (Eq. (9)). Once organic radicals are formed, residual hydrogen peroxide and hydroxyl radicals as well will contribute to mineralization through reactions (10) and (11). These issues highlight the importance of designing a proper oxidant feeding strategy that allows

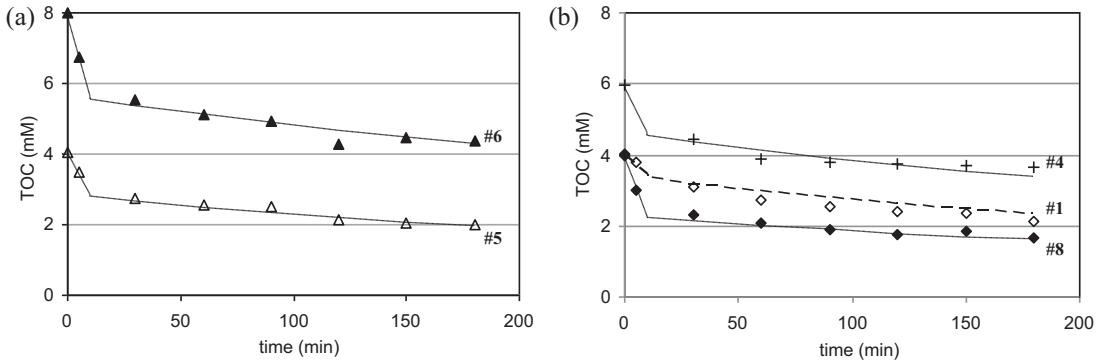

Fig. 5. Experimental and predicted TOC profiles.

Table 3
Explored conditions and outcomes attained at 180 min. Fe_0^{2+} = 0.46 mM, OG_0 = 0.25 mM.

Run #	Multiple H_2O_2 dosage	T (°C)	% Fe precipitated	ε
15	6 mM (0′) + 6 mM (30′)	25	–	5.6
16	6 mM (0′) + 3 mM (30′) + 3 mM (90′)	25	–	4.4
17	6 mM (0′) + 6 mM (30′)	50	–	3.2

an overall improvement of mineralization and efficiency in Fenton process.

The sequential addition of H_2O_2 on Orange G degradation was tested at the conditions listed in Table 3. Experiment #1 was selected as a reference, so the total oxidant addition equalled a concentration of 12 mM. In these stepwise experiments, the hydrogen peroxide was added in different aliquots but the first dose was fixed (6 mM), a value high enough to ensure instantaneous discoloration and a proper initial mineralization rate as shown in Fig. 2b. Fig. 6 presents the TOC concentration profiles for experiments with multiple H_2O_2 doses, while Fig. 7 shows the corresponding DO profiles. TOC Profiles attained with a single dose of 12 mM at 25 °C and 50 °C (experiments #1 and #8) have been included to help in the analysis. The effect of the stepwise oxidant addition on Fenton oxidation seems to depend on the concentration of H_2O_2 added in each step, the number of doses and the temperature. The highest mineralization was attained in experiment #15, in which 6 mM of H_2O_2 was added twice (at 0 and at 30 min) at 25 °C. In this case, oxidant is not completely consumed within the 180 min (not shown). The addition of a second step of H_2O_2 favors the oxidation of the intermediate products through reactions 10 and 11. Moreover, efficiency calculated for experiment #15 indicates an improvement of 43% over the unique dose experiment at 25 °C. Under these conditions, the sequential formation of the hydroxyl radicals seems to reduce the extent of parasitic reactions and benefits the efficiency.

As an attempt to further improve these outcomes, the oxidant was added in three doses of 6, 3 and 3 mM (experiment #16), but no enhancement was achieved. After the second dose, mineralization as well as oxygen production rates slowly progress. After the third dose, mineralization is halted and DO increases appreciably (as shown in Fig. 7), suggesting that only parasitic reactions are promoted. Thus, efficiency is only enhanced in 11% with respect to the reference experiment (Table 3).

Finally, hydrogen peroxide dosification was investigated at 50 °C in experiment #17. The oxidant initially added (6 mM) is fully depleted within the first 30 min (Fig. 3b). The second step of H_2O_2 is added at 30 min and a slight improvement in TOC consumption is observed. After addition of the second dose, a marked increase in oxygen concentration is observed (Fig. 7) suggesting that the added oxidant is mostly consumed by parasitic reactions. After 90 min, the oxidant is again completely consumed and mineralization ends. Comparing experiments #15 and #17, it arises that it is not always advisable to combine intensification through temperature increase and step addition.

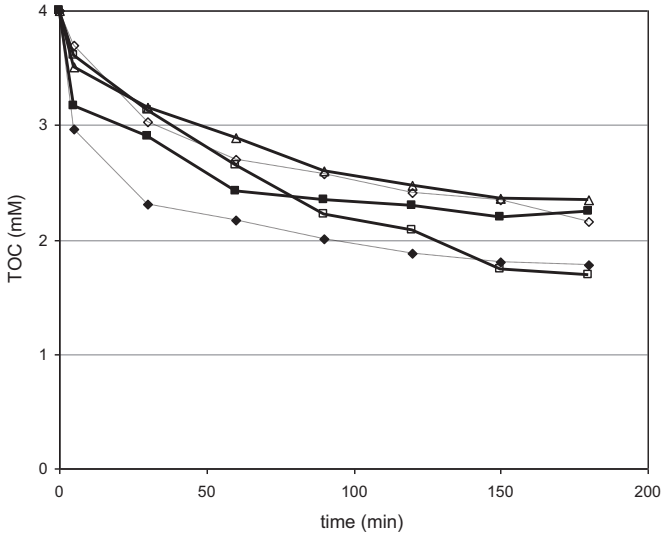

Fig. 6. TOC concentration against time at 25 °C (empty symbols) and 50 °C (solid symbols) under air flow rate. OG_0 = 0.25 mM; (-◇-, -◆-) runs #1 and #8; (▭, ▬) runs #15 and #17; (-△-) run #16.

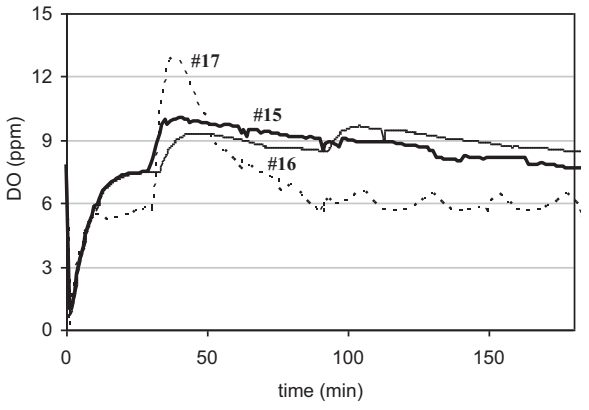

Fig. 7. DO against time for experiments with multiple oxidant doses.

Results are noteworthy since they indicate that, under certain conditions, TOC conversion and oxidant efficiency can be enhanced simultaneously; an outcome never achieved with single dose experiments. Dosification parameters (number of doses, oxidant concentration dose and temperature) should be carefully selected. Neither the depletion of the oxidant nor the addition of many small doses is apparently appropriate, since they affect notoriously the mineralization.

4. Conclusions

The homogeneous Fenton process is investigated under different operating conditions with the azo dye Orange G as a model compound. The effect of initial dye, oxidant and catalyst concentrations, and of temperature, on the discoloration, mineralization, oxidant consumption, dissolved oxygen concentration and efficiency is addressed. Within the range of conditions studied, the solution is instantaneously discolorized and partially mineralized. A lumped two-stage model is proposed which predicts satisfactorily the evolution of mineralization in Orange G Fenton oxidation.

Temperature is a key parameter to enhance mineralization, provided the oxidant concentration used is at or beyond the stoichiometric dose. However, as reaction temperature is enhanced, scavenger reactions are also enhanced and the oxidant could be less efficiently used.

The sequential addition of hydrogen peroxide can enhance both mineralization and efficiency. In single dose experiments, best oxidant efficiency and mineralization is attained when an adequate amount of hydroxyl radicals are generated during the first minutes and they are used to attain complete and instantaneous discoloration. At this point, many organic radicals are formed and they will react with residual hydrogen peroxide and hydroxyl radicals to achieve mineralization.

DO below solubility is not recommended; intermediates organic molecules continue suffering degradation but additional mineralization is not promoted. In such cases, additional doses of hydrogen peroxide could help to achieve further mineralization. Neither the depletion of the oxidant before addition of a second dose/step nor many small doses appear to be beneficial for further improving the mineralization. Dosification parameters (number of doses, oxidant concentration dose and temperature) should be carefully selected. Further experimental and modeling efforts concerning the stepwise addition of the oxidant is required to better understand the involved phenomena and thus, find optimal operating conditions.

Acknowledgements

Financial support from CONICET, UBA, UNMdP and ANPCyT are gratefully acknowledged. We want to express our gratitude to C. Rodriguez and H. Asencio for their technical support. The authors would also like to thank the reviewers for their careful reading and helpful comments.

References

[1] H. Zollinger, Color Chemistry-Syntheses, Properties and Applications of Organic Dyes and Pigments, VCH Publishers, New York, 1991.
[2] C. Bouasla, M.E.-H. Samar, F. Ismail, Desalination 254 (2010) 35–41.
[3] I.K. Konstantinou, T.A. Albanis, Applied Catalysis B: Environmental 49 (2004) 1–14.
[4] I. Oller, S. Malato, J.A. Sánchez-Pérez, Science of the Total Environment 409 (2011) 4141–4166.
[5] P.R. Gogate, A.B. Pandit, Advances in Environmental Research 8 (2004) 501–551.
[6] E. Neyens, J. Baeyens, Journal of Hazardous Materials 98 (2003) 33–50.
[7] E. Lipczynska-Kochany, G. Sprah, S. Harms, Chemosphere 30 (1995) 9–20.
[8] Y. Du, M. Zhou, L. Lei, Water Research 41 (2007) 1121–1133.
[9] J. Sun, S. Sun, G. Wang, L. Qiao, Dyes and Pigments 74 (2007) 647–652.
[10] L. Santos-Juanes, J.L. García Sánchez, J.L. Casas López, I. Oller, S. Malato, J.A. Sánchez Pérez, Applied Catalysis B: Environmental 104 (2011) 316–323.
[11] H. Zhang, H.J. Choi, C. Huang, Journal of Hazardous Materials 125 (2005) 166–174.
[12] R.C. Martins, A.F. Rossi, R.M. Quinta-Ferreira, Journal of Hazardous Materials 180 (2010) 716–721.
[13] E. Yamal-Turbay, M. Graells, M. Pérez-Moya, Industrial and Engineering Chemistry Research 51 (2012) 4770–4778.
[14] B. Utset, J. Garcia, J. Casado, X. Domenech, J. Peral, Chemosphere 41 (2000) 1187–1192.
[15] L. Prieto-Rodríguez, I. Oller, A. Zapata, A. Agüera, S. Malato, Catalysis Today 161 (2011) 247–254.
[16] C.K. Duesterberg, W.J. Cooper, T.D. Waite, Environmental Science and Technology 39 (2005) 5052–5058.
[17] I. Arslan Alaton, S. Teksoy, Dyes and Pigments 73 (2007) 31–39.
[18] J.H. Ramirez, F.M. Duarte, F.G. Martins, C.A. Costa, L.M. Madeira, Chemical Engineering Journal 148 (2009) 394–404.
[19] Y. Wu, S. Zhou, K. Zheng, X. Ye, F. Qin, Waste Management 31 (2011) 468–474.
[20] American Society of Civil Engineers, Measurement of Oxygen Transfer in Clean Water, ASCE Publications, USA, 1993.
[21] S. Sun, C. Li, J. Sun, S. Shi, M. Fan, Q. Zhou, Journal of Hazardous Materials 161 (2009) 1052–1057.
[22] H. Gallard, J. de Laat, B. Legube, New Journal of Chemistry 22 (1998) 263–268.
[23] J.H. Ramirez, C.A. Costa, L.M. Madeira, Catalysis Today 107–108 (2005) 68–76.
[24] A.A. Burbano, D.D. Dionysiou, M.T. Suidan, T.L. Richardson, Water Research 39 (2005) 107–118.
[25] A. Bach, H. Shemer, R. Semiat, Desalination 264 (2010) 188–192.
[26] J.A. Zazo, G. Pliego, S. Blasco, J.A. Casas, J.J. Rodríguez, Industrial and Engineering Chemistry Research 50 (2011) 866–870.
[27] R Core Team, R: A Language and Environment for Statistical Computing, R Foundation for Statistical Computing, Vienna, Austria, 2012 http://www.R-project.org